

# Telotristat Etiprate alleviates rheumatoid arthritis by targeting LGALS3 and affecting MAPK signaling

Ling Zhang<sup>§</sup>, Yanwen Lin<sup>§</sup>, Xinrui Xu, Huihui Liu, Xiangyu Wang, Jihong Pan\*

Biomedical Sciences College & Shandong Medicinal Biotechnology Centre, Shandong First Medical University & Shandong Academy of Medical Sciences; Key Lab for Biotech-Drugs of National Health Commission, Ji'nan, Shandong, China.

**SUMMARY** Rheumatoid arthritis (RA) is one of the most widespread chronic immune-mediated inflammatory diseases characterized by continuous erosion of bone and cartilage by synovial hyperplasia. Telotristat Etiprate is an inhibitor of tryptophan hydroxylase, a rate-limiting enzyme in the biosynthesis of serotonin. Telotristat Etiprate can be used in the treatment of carcinoid syndrome. The purpose of this study was to explore the effect of Telotristat Etiprate on RA and its mechanism. We investigated Telotristat Etiprate in collagen-induced arthritis (CIA) model mice and in rheumatoid arthritis synovial fibroblasts (RASFs). Results showed that Telotristat Etiprate had anti-inflammatory effects both *in vitro* and *in vivo*, can inhibit the invasion and migration of cells, inhibit the formation of pannus, and induce cell apoptosis. Transcriptome sequencing (RNA-seq) and mass spectrometry analysis showed that Galectins-3 (LGALS3) could be a newly identified target of Telotristat Etiprate, affecting the phosphorylation of the MAPK signaling pathway through UBE2L6, thereby improving RA.

**Keywords** rheumatoid arthritis, Telotristat Etiprate, LGALS3, MAPK signaling pathway, UBE2L6

## 1. Introduction

Rheumatoid arthritis (RA) is a chronic, inflammatory, destructive, systemic autoimmune disease characterized by synovial hyperplasia and leukocyte exudation leading to joint destruction (1,2). Rheumatoid arthritis synovial fibroblasts (RASFs) are major components of vascular membrane proliferation and actively participate in joint inflammation and cartilage and bone destruction through contact interactions, and production of inflammatory mediators and matrix degrading enzymes (3). RASFs resist apoptosis, exhibit more adhesion and invasion properties, evade contact inhibition, cells migrate and colonize elsewhere, infiltrate, and destroy joints in immunodeficient mice (4-6). Notably, this aggressive phenotype persisted after multiple cell passages *in vitro*, suggesting that synovial fibroblasts in RA were persistent, if not irreversible. The joints of RA patients produce excessive amounts of inflammatory molecules, such as cytokines and matrix metalloproteinases, which promote the destruction of cartilage and bone (7,8).

The goal of RA treatment is to minimize symptoms such as pain and swelling, prevent skeletal deformities, and maintain daily function. However, RA is currently mainly treated with anti-rheumatic drugs (DMARDs),

which are painkillers used to help reduce pain (9). DMARDs have been found to improve symptoms, reduce joint damage, are usually started early in the disease and can help about half of people get remission, improving overall prognosis. However, due to the lack of long-term experience in the use of these drugs, which can only relieve but not treat the pain, the treatment process is often accompanied by a large number of toxic side effects (10). Therefore, we urgently need to find a small molecule inhibitor for targeted improvement of RA, from analgesia to pain treatment, and fundamentally relieve the pathological symptoms of RA.

Due to synovial hyperplasia, bone and cartilage are constantly eroded, leading to the increase of some pro-inflammatory cells (such as macrophages, plasma cells, B cells, T cells, *etc.*), which activate NF-KB, MAPK, JAK/STAT, PI3/Akt/mTOR and other inflammatory signaling pathways, and produce a large number of inflammatory cytokines (IL-6, IL-8, IL-1 $\alpha$ , IL-1 $\beta$ , CCL2). Based on the above inflammatory signaling pathways, we purchased 1092 inhibitors from selleck's inhibitor library for screening. After layer upon layer screening, we finally selected Telotristat Etiprate, which had the greatest inhibitory effect, and further explored its mechanism of action to provide a theoretical basis

for RA treatment. Telotristat Etiprate is an inhibitor of tryptophan hydroxylase, a rate-limiting enzyme involved in 5-HT biosynthesis (11,12). The US Food and Drug Administration and the European Commission recently approved Telotristat Etiprate. This is a Category 2A recommendation in the National Comprehensive Cancer Network's Clinical Practice Guidelines for treating Carcinoid syndrome (CS) diarrhea that is inadequately controlled by Somatostatin Analogs (SSA) therapy (13).

In this study, first, collagens induced arthritis (CIA) model mice were used to explore whether Telotristat Etiprate has any effect on RA. Next, the effect of Telotristat Etiprate treatment on the biological function of RASFs was detected *in vitro*, and the mechanism of its action was explored by RNA-seq and mass spectrometry, thus providing a basis for the treatment of RA.

## 2. Materials and Methods

### 2.1. Collection of synovial tissues

Synovial tissues were collected during knee joint replacement surgery from patients with RA ( $n = 14$ ; five males, nine females, aged 35 to 75 years, mean age of 55 years). Synovial tissues used in this study were provided by the Shandong Provincial Hospital. All patients fulfilled the 1987 American College of Rheumatology revised criteria for RA diagnosis. Written informed consent was obtained from each patient, and all samples were de-identified for research use. The Ethical Committee of the Shandong Academy of Medicinal Sciences approved this study (approval number 2019-02).

### 2.2. Collagen-induced arthritis (CIA) model

The CIA model is a well-established mouse model for human RA. The CIA model was induced by tail injection of 9-week-old male mice with 2 mg/mL bovine type II collagen (Chondrex, Washington, USA) and complete Freund's adjuvant (Sigma-Aldrich, Mannheim, Germany) 1:1 emulsifier (200  $\mu$ L). After 21 days, the mouse tails were injected with bovine type II collagen and Sigma-Aldrich 1:1 emulsifier (200  $\mu$ L). Mice were monitored for arthritis symptoms once a day. After swelling was identified in all four paws, mice were treated with Telotristat Etiprate for 1 month (intraperitoneal injection, 20 mg/mL), and paw inflammation relief was observed and recorded. Scores were based on the degree of swelling and erythema around the joint, ranging from 0 to 3, no signs of erythema or swelling; 1, erythema in only one joint; 2, erythema and swelling areas found in only one joint; 3, severe erythema and swelling extending from one joint to both joint areas. The total score for each mouse was added to the four paw scores, and the maximum possible score for each mouse was 12 points.

### 2.3. Cell acquisition and stimulation

Synovial tissue was soaked and digested with type II and III collagenase at 37°C for 6–8 h in 5% CO<sub>2</sub>. Cells were cultured in DMEM (Gibco) complete medium containing 15% fetal bovine serum (FBS) and 1% penicillin/streptomycin and were used in passages from 3 to 7 generations.

We screened a number of commonly used inflammatory factors for RASF stimulation, including lipopolysaccharide (LPS), IL-1 $\beta$ , IL-1 $\alpha$ , IL-6, and TNF- $\alpha$ , but multiple trials found that IL-1 $\beta$  stimulation was most effective. RASFs were inoculated on cell culture plates and stimulated with IL-1 $\beta$  (10 ng/mL) for 24 h. Telotristat Etiprate was dissolved in 1 mM DMSO to reach a final concentration of 50 ng/mL in DMEM complete medium.

### 2.4. RNA extraction and qRT-PCR

Total RNA was extracted from cultured cells using Trizol reagent (Invitrogen) according to the reagent instructions, and RNA was reverse transcribed into cDNA using HiScript II Q RT SuperMix for qPCR (Vazyme). qRT-PCR was performed using a LightCycler 480 (Roche, Basel, Switzerland) according to the following protocol: pre-denaturation at 95°C for 10 min, denaturation at 95°C for 15 s, and annealing/extension at 60°C for 1 min for 40 cycles. Upstream primers and downstream primers are shown in Table 1. All primers were synthesized by Beijing Genomics (Beijing, China). Each sample was analyzed in triplicate, and expression changes of target genes were calculated by the 2<sup>- $\Delta\Delta$ Ct</sup> relative quantitation method.

### 2.5. ELISA

Cells were treated with Telotristat Etiprate or DMSO. After 6 h, the proinflammatory factor IL-1 $\beta$  was added for stimulation. After 24 h, the supernatant was collected, and the secretion of IL-6, IL-8, and CCL2 was detected by ELISA (MultiSciences). After drug treatment in mice, serum was collected, debris was removed by centrifugation, and the secretion of inflammatory factors, such as IL-6, IL-8, IL-1 $\alpha$ , and COMP, was detected by ELISA.

### 2.6. *In vitro* cell invasion and migration assay

After diluting matrix glue with serum-free and antibiotic-free DMEM at a ratio of 1:7, 100  $\mu$ L were added to the upper chamber of the TransWell (each chamber) and incubated at 37°C with 5% CO<sub>2</sub> for 1 h. RASFs were treated as described above and inoculated with 10,000 cells in the TransWell upper chamber (DMEM complete medium with 2% FBS), and complete medium containing 15% FBS was added to the surface of the

**Table 1. Primers used for qRT-PCR**

Primer name <sup>†</sup>	Primer base sequence (5'to 3')
GAPDH	Forward: TGATGACATCAAGAAGGTGG Reverse: TTA CTCTGGAGGCCATGT
IL-6	Forward: CCACCGGAACGAAAGAGAA Reverse: GAGAAGGCAACTGGACCGAA
IL-8	Forward: CAGTTTTGCCAAGGAGTGCTAA Reverse: AACTTCTCCACAACCCTCTGC
CCL2	Forward: AGAGGCTGAGACTAACCAGAA Reverse: TTTTCATGCTGGAGGCGAGAG
IL-1 $\alpha$	Forward: AGATGCTGAGATACCCAAAACC Reverse: CCAAGCACACCCAGTAGTCT
IL-1 $\beta$	Forward: ATGATGGCTTATTACAGTGGCAA Reverse: GTCGGAGATTTCGTAGCTGGA
PDGFRL	Forward: CAAGAACAAGCGTCCAAAAGAAC Reverse: AGCGACCTTTATCCAGCACTT
PLAT	Forward: AGCGAGCCAAGGTGTTTCAA Reverse: CTTCCAGCAAATCCTTCGGG
LGALS3BP	Forward: AGGTACTTCTACTCCGAAGGA Reverse: GGCCACTGCATAGGCATAACA
HSPB3	Forward: ATAGAGATTCCAGTGCCTTACCA Reverse: CAGGCAGTGCATATAAAGCATGA
CD274	Forward: GGACAAGCAGTGACCATCAAG Reverse: CCCAGAATTACCAAGTGATGCTCT
UBE2L6	Forward: TGGACGAGAACGGACAGATTT Reverse: GGCTCCTGATATTCGGTCTATT
OAS1	Forward: AGCTTCGTA CTGAGTTCGCTC Reverse: CCAGTCAACTGACCCAGGG
NR4A1	Forward: ATGCCCTGTATCCAAGCCC Reverse: GTGTAGCCGTCCATGAAGGT
BATF2	Forward: CACCAGCAGCAGAGTCTC Reverse: TGTGCGAGGCAAACAGGAG
ANGPTL1	Forward: AGAAAGGAAAGCCGTAACATGAA Reverse: TCCTGTATCTTGTGGCCATCT
HERC5	Forward: ATGGGCTGCTGTTACTTTCC Reverse: TTCCAGTTGTCCATCTTTTCC
OASL	Forward: CTGATGCAGAACTGTATAGCAC Reverse: CACAGCTCTAGCACCTCTT
RSAD2	Forward: CAGCGTCAACTATCACTTCACT Reverse: AACTCTACTTTGCAGAACCTCAC

<sup>†</sup>All primers are targeted against human genes.

lower chamber. After 18 h of incubation, cells invading the lower surface were stained and counted (three repeat views for each treatment condition) to calculate the average number of invaded cells.

RASFs were inoculated in six-well plates and treated in accordance with the above methods. After 24 h, RASF medium was replaced with serum-free and antibiotic-free medium and cell scratching was performed. RASF migration was recorded at 0, 3, 6, 12, and 24 h.

### 2.7. Apoptosis was detected by flow cytometry

In brief, RASFs were treated as described above, digested with trypsin, stained with Annexin V-fluorescein isothiocyanate (FITC) (10  $\mu$ g/mL), and propidium iodide (10  $\mu$ g/mL) (Sigma) according to manufacturer's protocol and analysed with a FACSCalibur machine (BD Biosciences). Annexin V+/+ cells were considered apoptotic cells.

### 2.8. Apoptosis was detected by TUNEL assay

The TUNEL method was used to detect RASF apoptosis. Cells in good condition were inoculated into 96-well plates for drug treatment, washed with PBS three times (3 min each), fixed with 4% paraformaldehyde, and permeabilised with 0.2-0.5% Triton X-100. Cells were then stained with TUNEL and DAPI and immediately observed under a confocal fluorescence microscope. Green fluorescence (apoptotic cells) was observed at 520 nm, and DAPI blue fluorescence was observed at 460 nm. Each group was set up with two repeating holes, and the experiment was repeated three times.

### 2.9. Histological analysis

A micro-CT system (Quantum GX, USA) was used to scan mouse paws, observe the joint microstructure, and accurately analyse the same area of mouse joints. After immobilisation in 4% paraformaldehyde for 24 h, claws were decalcified in 15% ethylenediamine tetraacetic acid (EDTA) for about a month. Claws were embedded in paraffin and cut into 5- $\mu$ m sagittal sections. The sections were stained with H&E and Safranin O-Fast Green FCF.

### 2.10. Western blotting analysis

Cells were collected and lysed with RIPA lysate and protease inhibitors. The cleavage materials were separated by electrophoresis through sodium dodecyl sulfate-polyacrylamide gel electrophoresis (SDS-Page) and transferred to a PVDF membrane with a pore size of 0.45 $\mu$ m. Then, western blotting was performed with a specific primary antibody and incubation was conducted overnight at 4°C. After washing with TBST, the membrane was incubated with each corresponding secondary antibody at 37°C for 1h and detected using ECL Plus detection system (Thermo Scientific, Pittsburgh, PA, USA). The following primary antibodies were used in this experiment: anti-P38 MAPK, anti-P44/42 MAPK, anti-SAPK/JNK MAPK, anti-P65 NF-KB, phospho- P38 MAPK, phospho-P44/42 MAPK, phospho-SAPK/JNK MAPK, phospho-P65 NF-KB, anti-PLD3, anti-LGALS3, anti-YKL140, anti-YWHAG, anti-CD11C, anti-CASP3, anti-PRDX3, anti-RAS2, anti-CASP3, anti-DNAJA1.

### 2.11. Immunofluorescence microscopy

After RASFs were treated in 48-well plates, the cells were slowly washed with PBS 3 times (3 min each), and fixed with 4% paraformaldehyde. After rinsing with PBS 3 times (3 min each), the RASF cells were sealed with 5% bovine al-bumin (BSA) for 1h at 37°C, and the cells were incubated with specific monoclonal antibodies at 4°C overnight. After rinsing with PBS 3 times, the fluorescence secondary antibody was incubated and the nuclei were stained with 4',6'-Diamidino-2-phenylindole (DAPI).

## 2.12. Small interfering RNA (siRNA) and adenovirus transfection and RNA sequencing

SiRNA and negative control were derived from RuiboBio (Guangzhou Development Zone, Pennant District, Guangzhou, China). SiRNA and negative controls were transfected into RASFs using the HiPerFect co-transfection reagent, following manufacturer's instructions. The sequence of siRNA was designed and synthesized by RuiboBio (Guangzhou, China), and the most effective sequence (as shown in Table 2) was used in the following experiment. RASFs ( $8 \times 10^4$  cells cultured in 6-well plates or  $2 \times 10^4$  cells cultured in 24-well plates) were infected with UBE2L6 adenovirus or Empty adenovirus by ADV-HR (ViGeneBiosciences) as per manufacturer's instructions. For RNA sequencing, TNF- $\alpha$  and IL-1 $\beta$  stimulation after Telotristat Etiprate treatment for 24 h, total RNA was collected by Trizol method to construct a cDNA library for RNA transcriptomic sequencing by IC-Bio Technologies Co., Ltd (Hangzhou, Zhejiang, China). Gene Ontology (GO) enrichment analysis and Kyoto Encyclopaedia of Genes and Genomes (KEGG) pathway enrichment analysis were used to evaluate the bioactivity and signaling pathway distribution of differentially expressed Genes (DEGs).

## 2.13. Drug affinity responsive target stability (DARTS) assay and mass spectrometry (MS)

The tissues of RA patients (1.5 to 2.5g) were ground in liquid nitrogen and lysed on ice for 20 minutes with t-Per<sup>TM</sup> histone extraction kit (Thermo Scientific, Waltham, MA, USA) containing protease and phosphatase inhibitors. 10 X TNC buffer (1M Tris-HCl, 5mL; 5M NaCl, 1mL; 1M CaCl<sub>2</sub>, 1mL; double distilled water, 3mL; pH7.4) was added to the cell lysate (total protein 5 mg/mL), to the desired concentration, and gently stirred. Telotristat Etiprate and protein lysates were incubated at room temperature for 1h to fully bind the target protein to the ligand, then treated with protease (dissolved in a 1 X TNC buffer) at a ratio of 1:100, 1:500, 1:1,000, 1:2,500, 1:5,000 (wt/wt), and digested at room temperature for 15 minutes. After the protein lysis products were incubated with drugs and digested by protease, 5 X protein loading buffer was added before boiling for 5-7 min. SDS-PAGE and Coomassie bright blue staining showed the bands. Finally, the gels with obvious changes were analyzed by

MASS spectrometry (BGI, Beijing, China).

## 2.14. Statistical analysis

Data analysis was performed by two-factor analysis of variance (ANOVA), followed by Bonferroni's multiple comparison test performed using GraphPad Prism 7 software (La Jolla, CA, USA). Results were expressed as the mean  $\pm$  SEM of five different experiments. The differences in central tendency were statistically significant. Results were considered statistically significant at a *p* value of  $< 0.05$ ; \* *p*  $< 0.05$ , \*\* *p*  $< 0.01$ , and \*\*\* *p*  $< 0.001$ , respectively.

## 3. Results

### 3.1. Improvement of inflammatory phenotype in collagen-induced model mice treated with Telotristat Etiprate

To establish an animal model of CIA, arthritis was induced in DBA/1J mice and treated by intraperitoneal injection of Telotristat Etiprate (20 mg/mL) once every day for a month. We included the following three groups: mice without CIA induction (*n* = 6), mice that did not receive drug treatment after CIA induction (*n* = 6), and mice that received drug treatment after CIA induction (*n* = 6). Two observers measured the degree of paw swelling daily and assigned a score (Figure 1, A and B). As shown in Figure 1C, the difference between front and rear paws was significant before and after treatment (swelling subsided and erythema decreased). Serum was obtained from fresh blood, and the expression of IL-6, IL-8, IL-1 $\alpha$ , and COMP was detected by ELISA. We found that the expression of serum inflammatory factors after Telotristat Etiprate treatment was significantly reduced (Figure 1D). Micro-computed tomography (micro-CT) was used to image mouse paws, and it was evident that the joints of treated mice were significantly improved compared with those of the untreated mice (Figure 1F) This also, showed that trabecular separation (Tb.Sp, mm) was reduced, and trabecular thickness (Tb.Th, mm) and the bone volume to bone volume fraction (BV/TV, %) rise were exported for reconstruction using the manufacturer's software, Caliper Analyze (Figure 1E). Finally, aematoxylin and eosin (H&E) (Figure 1G) and Safranin O-Fast Green FCF (Figure 1H) staining and analysis demonstrated an improvement in synovial hyperplasia, monocyte infiltration, and bone destruction in mice treated with Telotristat Etiprate.

### 3.2. Telotristat Etiprate improves the arthritic phenotype of RASFs after treatment

To investigate the role of Telotristat Etiprate in RA, we first analysed the expression and secretion of inflammatory factors in RASFs, as RA is characterised by

**Table 2. siRNA sequences**

siRNA name <sup>†</sup>	sequence (5'to 3')
NR4A1	GGGACTGGATTGACAGTAT
LGALS3BP	GGACCTGTATGCCTATGCA
UBE2L6	GCTGGTGAATAGACCGAAT
HSPB3	GCACGGTTTTATCTCAAGA
PDGFRL	GCACCAAAGACGCGAGTCTA

<sup>†</sup>All sequences are targeted against human genes.

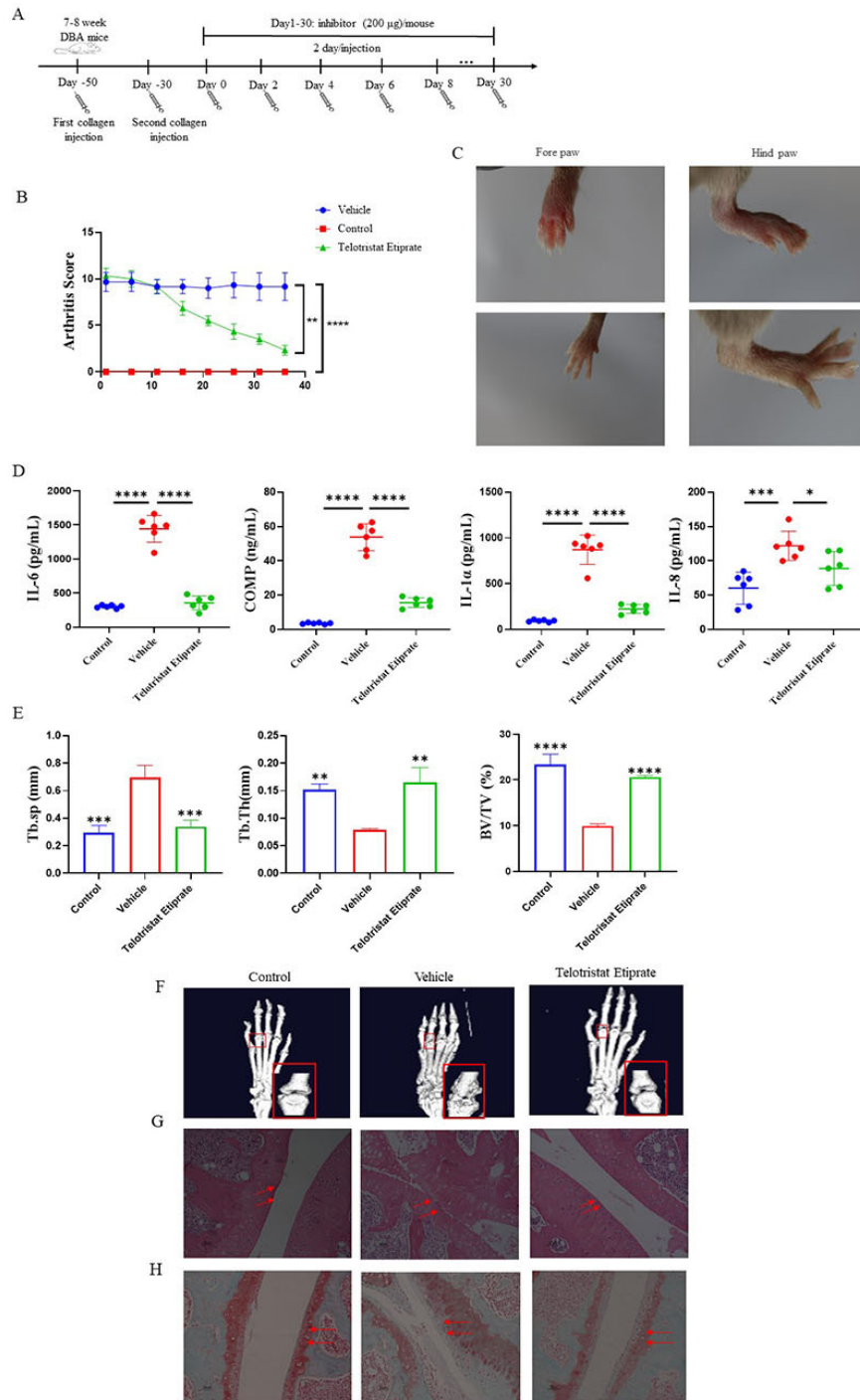


**Figure 1. Improvement of inflammatory phenotype in collagen-induced model mice treated with Telotristat Etiprate.** The following three groups were studied: 1. Contro group: mice without CIA induction ( $n = 6$ ); 2, Vehicle group: mice injected with DMSO as control after CIA induction but not treated with Telotristat Etiprate ( $n = 6$ ); 3, Telotristat Etiprate group, mice treated with Telotristat Etiprate after CIA induction ( $n = 6$ ). (A) The overall scheme of animal experiments. (B) Two observers rated paw swelling (0-3 for each paw) on the first day of treatment after induction of arthritis. (C) Changes in swelling degree of paw (hind paw and fore paw) of mice before and after treatment. (D) Serum was extracted from fresh blood of mice, and the secretion of inflammatory cytokines in serum was detected by ELISA (IL-6, IL-8, IL-1 $\alpha$ , COMP). (E) Analysis of mouse paws by micro-CT, trabecular separation (Tb.Sp, mm), trabecular thickness (Tb.Th, mm) and the bone volume to bone volume fraction (BV/TV, %). (F) Micro-CT imaging showed significant improvement in the degree of joint damage in the treated mice. (G) and (H) The histological changes of the joint were detected by HE staining and Muscovy solid green staining. All results are presented as the mean  $\pm$  SEM of three independent experiments performed in triplicate; \* $p < 0.05$ , \*\* $p < 0.01$ , \*\*\* $p < 0.001$ .

joint inflammation. After 6 h of treatment with different concentrations of Telotristat Etiprate (1, 10, 50, and 100 ng/mL), the proinflammatory factor IL-1 $\beta$  (10 ng/mL)

was added to stimulate the cells. After 24 h, the mRNA expression levels of *Il6*, *Il8*, and *Ccl2* were assessed (Figure 2, A and B). Cell survival rate was detected by

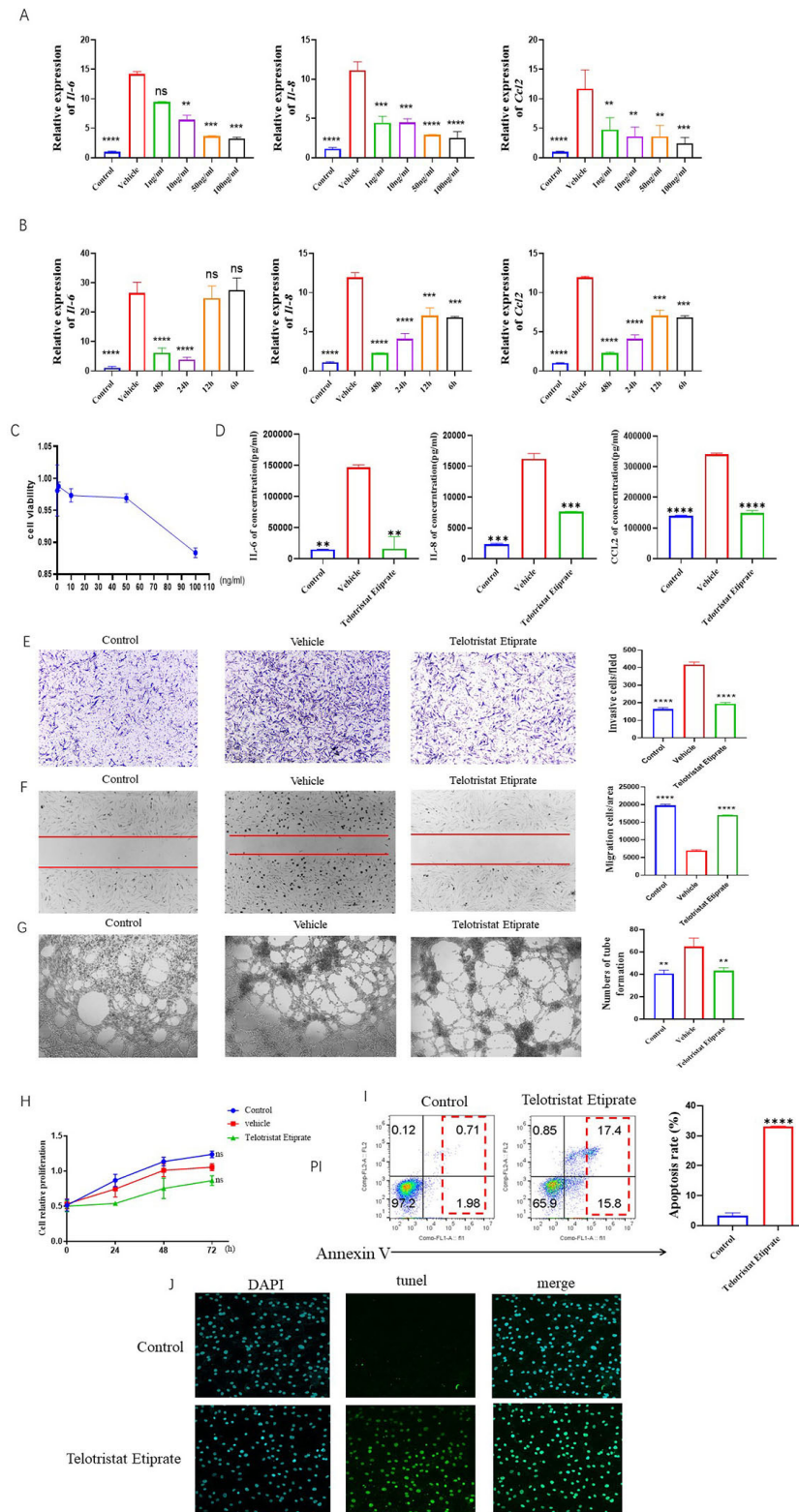


**Figure 2. Telotristat Etiprate improves the arthritic phenotype of RASFs after treatment.** (A) and (B) The optimal timing and concentration of drug action were investigated by qRT-PCR. (C) The survival rate of cells at different concentrations (0, 1, 10, 50, 100 ng/mL) was detected by CCK8 method. (D) After treatment with Telotristat Etiprate, cell supernatant was taken and the secretion of inflammatory cytokines (IL-6, IL-8, CCL2) was detected by ELISA. (E) Cell invasiveness was detected by the Transwell method. (F) Cell migration ability was detected by cell scratch method. (G) The effect of Telotristat Etiprate on RASF angiogenesis was detected by CRL-1730 cell assay. (H) The effect of Telotristat Etiprate on cell proliferation was detected by CCK8 assay. (I) Cell apoptosis was detected by flow cytometry. (J) TUNEL assay was used to further confirm Telotristat Etiprate induced apoptosis (green fluorescence). All results are presented as the mean  $\pm$  SEM of three independent experiments performed in triplicate; \* $p < 0.05$ , \*\* $p < 0.01$ , \*\*\* $p < 0.001$ .

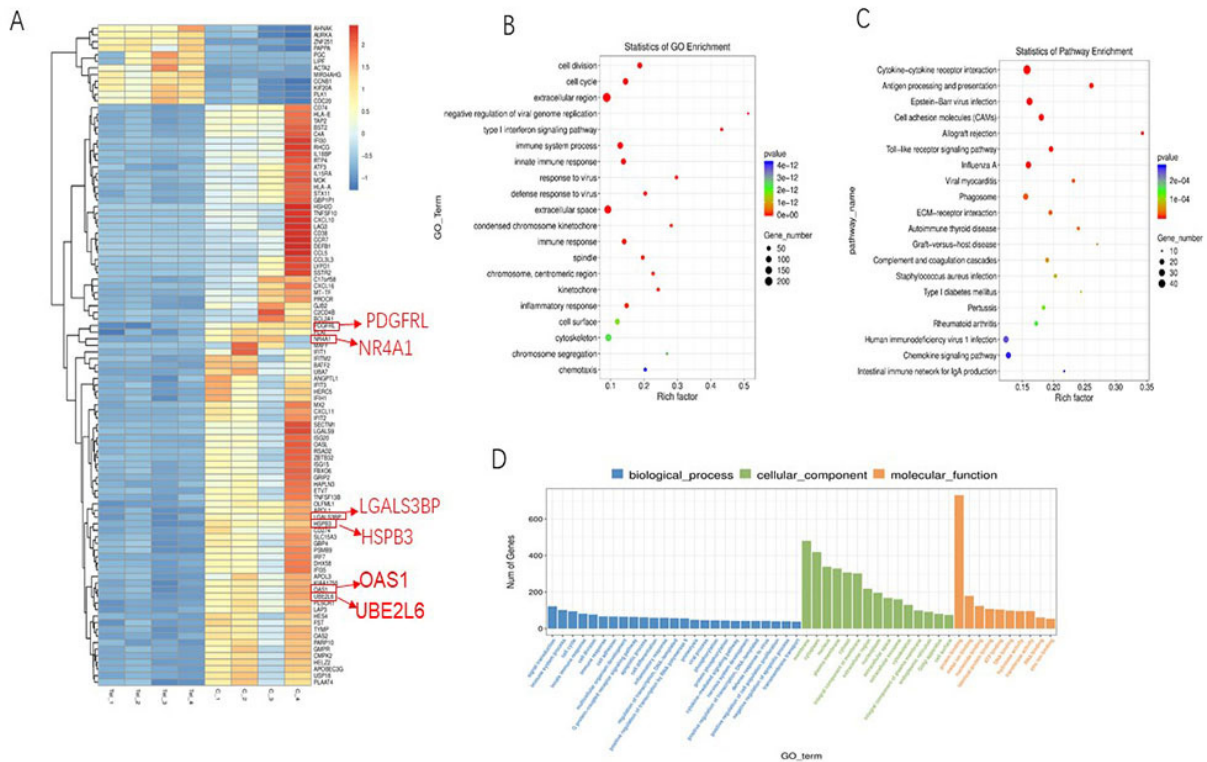


**Figure 3. RNA sequencing.** (A) Differentially expressed genes (DEGs) in Telotrlistat Etiprate treated RASFs activated by TNF- $\alpha$  and IL-1 $\beta$  were up-regulated in 562 genes and down-regulated in 597, of which the first 100 genes were significantly differentially expressed. (B) and (C) Enrichment analysis of GO classification and KEGG pathway was conducted. (D) In biological processes, 102 genes are involved in immune system processes, 82 genes are involved in endogenous immune responses, and 59 genes are involved in inflammatory responses.

the CCK8 method and was found to decrease when the drug concentration was 100 ng/ml (Figure 2C). However, the drug was most effective in inhibiting the expression of inflammatory cytokines and the cell survival rate was high when treated with 50 ng/mL for 24 h. The following experiments were carried out in accordance with this action time and concentration. In order to further explore the effect on the secretion of inflammatory factors in RASFs, supernatant from cells treated with the drug (50 ng/mL, 24 h) was tested for inflammatory cytokines (IL-6, IL-8, CCL2) by ELISA. The results showed that it also had a certain inhibitory effect on the secretion of inflammatory factors (Figure 2D).

RASFs not only secrete a large number of inflammatory factors but also have oncology characteristics and stronger invasion and migration abilities than normal synovial cells. To investigate the invasion and migration ability of RASFs treated with Telotrlistat Etiprate, we used the TransWell assay and cell scratch method. The results showed that the addition of Telotrlistat Etiprate did inhibit the invasion and migration of cells in the experimental group compared with the control group (Figure 2, E and F). In addition, in the presence of Telotrlistat Etiprate, RASFs also significantly decreased their angiogenesis promoting ability (Figure 2G).

Cell proliferation was detected by the CCK8 method, and Telotrlistat Etiprate treatment had no significant effect on cell proliferation (Figure 2H). Flow cytometry

and TUNEL method were used to detect the effect of Telotrlistat Etiprate on RASF apoptosis. Compared with the control group, the proportion of early apoptosis and late apoptosis in the experimental group after Telotrlistat Etiprate treatment was significantly increased (Figure 2I), which suggests that RASF apoptosis may be induced. In order to further verify, TUNEL method was also used to explore, as shown in Figure 2J. Compared with the control group, the apoptotic ability of Telotrlistat Etiprate was significantly enhanced (green fluorescence). It was further confirmed that Telotrlistat Etiprate may promote apoptosis of RASFs.

### 3.3. Telotrlistat Etiprate affects MAPK signaling pathway by inhibiting UBE2L6

Differentially expressed genes (DEGs), 562 up-regulated and 597 down-regulated, in Telotrlistat etiprate-treated RASFs activated by TNF- $\alpha$  and IL-1 $\beta$  were identified by RNA-seq analysis. The first 100 genes were significantly differentially expressed (Figure 3A). Then, enrichment analysis was performed for GO classification (Figure 3B) and KEGG pathway (Figure 3C). In biological processes, 102 genes are involved in immune system processes, 82 genes are involved in endogenous immune responses, and 59 genes are involved in inflammatory responses (Figure 3D). qRT-PCR was used to verify the significantly differentially expressed genes on the

heat map, and the results showed that after Telotristat Etiprate treatment, the expression of genes related to inflammatory immune response was reduced (Figure 4A). Interestingly, it was found that these genes with reduced expression were related to MAPK and NF-KB signaling pathways. Therefore, western blot was used to detect changes in phosphorylation levels of MAPK and NF-KB signaling pathways in Telotristat Etiprate treated cells. The results showed that the key proteins involved in MAPK signaling pathway, P38, P44/42 and SAPK/JNK, were phosphorylated. However, P65, a key protein involved in the NF-KB signaling pathway was not phosphorylated (Figure 4B). Therefore, we preliminarily believe that Telotristat Etiprate treatment can affect the change in the MAPK signaling pathway.

We selected from the genes in the MAPK signaling pathways that showed the greatest decrease in expression after Telotristat Etiprate treatment (*Lgals3bp*, *Na4a1*, *Hspb3*, *Pdgfr1*, *Ube2l6*). The expression of inflammatory cytokines (*Il-6*, *Il-8*, *Il-1 $\alpha$* , *Il-1 $\beta$* , *Ccl2*) at mRNA level was detected by qRT-PCR. The results showed that silencing these genes significantly reduced the expression of inflammatory cytokines compared with the control group. Among them, silencing UBE2L6 had the most significant inhibitory effect (Figure 4C). Next, ELISA (Figure 4D) and qRT-PCR (Figure 4E) were used to detect the effects of UBE2L6 overexpression or silencing (by adenovirus) on the expression and secretion of inflammatory cytokines (IL-6, IL-8, IL-1 $\alpha$ , IL-1 $\beta$ , CCL2) in cells. The results showed that, overexpression of UBE2L6 by adenovirus increases the expression and secretion of inflammatory cytokines, while silencing UBE2L6 causes a decrease. Preliminarily, it is considered that UBE2L6 can affect changes in the MAPK signaling pathway. To further explore, western blot was used to detect the phosphorylation of the MAPK signaling pathway after UBE2L6 was overexpressed or silenced by adenovirus. It was found that UBE2L6 could also cause phosphorylation of the MAPK signaling pathway after treatment. The effect was even more significant after IL-1 $\beta$  stimulation (Figure 4F). Therefore, we found that Telotristat Etiprate treatment in RASFs could affect the MAPK signaling pathway and inhibit the expression and secretion of inflammatory cytokines by inhibiting the expression of UBE2L6.

#### 3.4. LGALS3 is a new target of Telotristat Etiprate

To elucidate the molecular basis of Telotristat Etiprate's effect on RASFs, we isolated the protein portion bound to Telotristat Etiprate. Through the implementation of Drug Affinity Responsive Target Stability (DARTS) experiments and mass spectrometry, PLD3, LGALS3, YKL140, CD11C, CASP3, RRAS2, DNAJA1, PRDX3 and YWHAG were identified as potential candidates (Figure 5A). Then, using a series of the proportion of protease and cell lysis (1:100, 1, 500, 1:1,000, 1:2,500,

1:5,000) for the DARTS samples to conduct western blot analysis, Telotristat Etiprat was found to protect PLD3, LGALS3, CD11C and YWHAG (Figure 5B). Interestingly, we found that LGALS3 is involved in the MAPK signaling pathway processes. Therefore, we preliminarily concluded that Telotristat Etiprate plays a biological role by binding to target protein LGALS3.

#### 3.5. Telotristat Etiprate combine with LGALS3 to inhibit UBE2L6 and affect MAPK signaling pathway

In order to further explore the influence of LGALS3 on the MAPK signaling pathway, we used FHPI (0, 1, 10, 50, 100 ng/mL), an inhibitor of MAPK signaling pathway, and western blot method and found that the expression of LGALS3 decreased when the inhibitor FHPI was added. In addition, the inhibition effect was more significant when IL-1 $\beta$  was added (Figure 5C). Next, we further found through immunofluorescence that in the presence of MAPK inhibitor FHPI, the expression of LGALS3 decreased and also showed a concentration dependence (Figure 5D). Therefore, we believe that Telotristat Etiprate can affect the MAPK signaling pathway after binding to target protein LGALS3. Then, we further investigated whether LGALS3 could affect the expression and secretion of inflammatory cytokines in RASFs. qRT-PCR (Figure 5E) and ELISA (Figure 5F) experiments showed the expression and secretion of inflammatory cytokines in RASFs were decreased after silencing LGALS3, indicating that LGALS3 can indeed affect the expression and secretion of inflammatory cytokines in cells. In conclusion, Telotristat Etiprat can combine with target protein LGALS3 to inhibit UBE2L6 expression, thereby affecting the MAPK signaling pathway, inhibiting the expression of inflammatory cytokines in RASFs, and providing some relief of rheumatoid arthritis.

## 4. Discussion

Once a patient is diagnosed with rheumatoid arthritis, the overall treatment goal is to achieve a complete remission or at least a significant reduction in disease activity within approximately 6 months to prevent joint damage, disability, and systemic manifestations of rheumatoid arthritis (14,15). The importance of timely and targeted treatment of RA is highlighted by the fact that 80% of patients who are inadequately treated will develop a dislocated joint and 40% will be unable to work within 10 years of onset (16). The most common way to treat the disease is with anti-rheumatic drugs (DMARDs) (17,18). However, these drugs are not a complete cure and often cause serious side effects due to lack of long-term use experience. Fortunately, there is growing recognition that drugs can work by targeting multiple proteins. In addition, biological pathways and networks are abundant and powerful, so affecting only a single target can easily

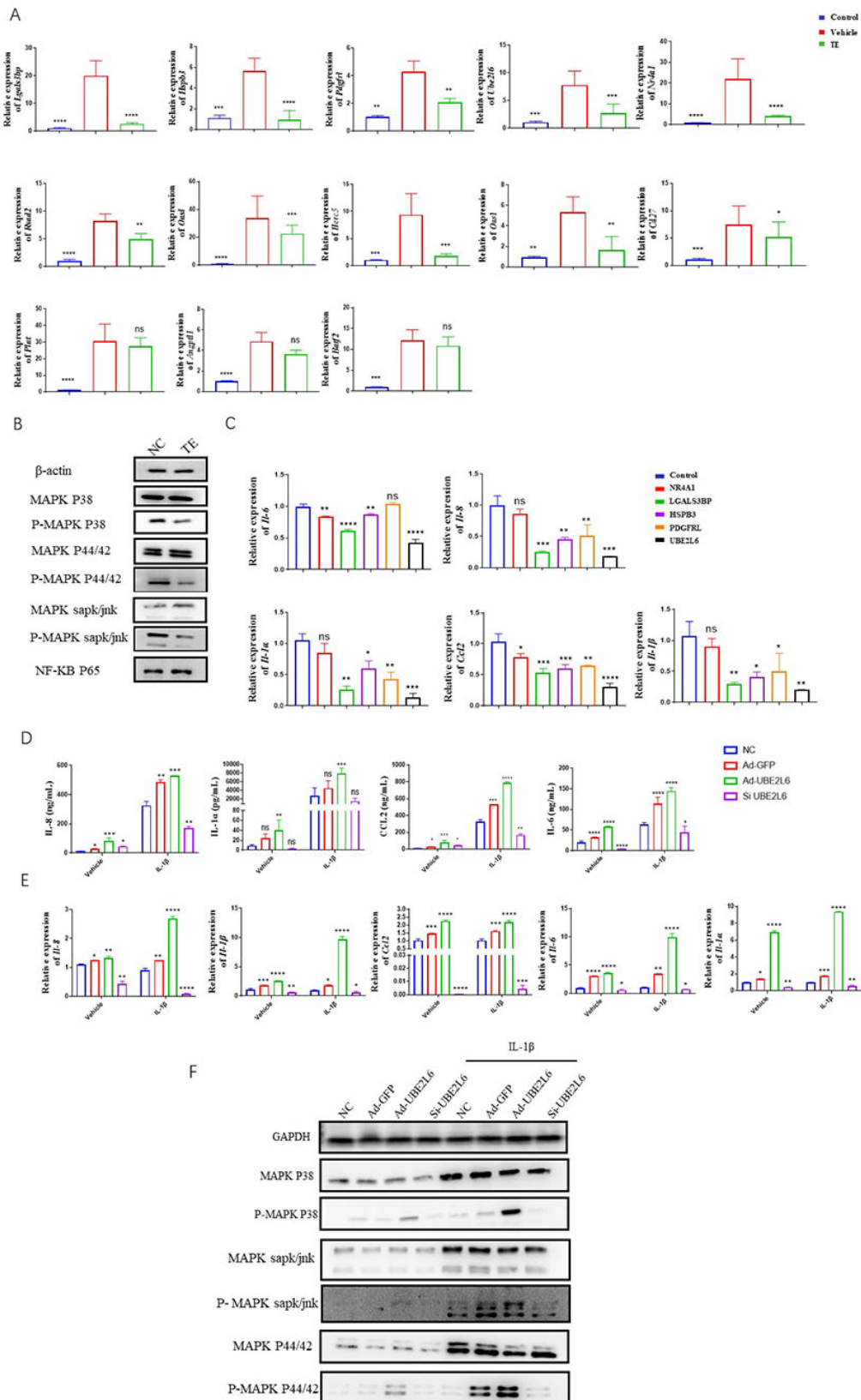
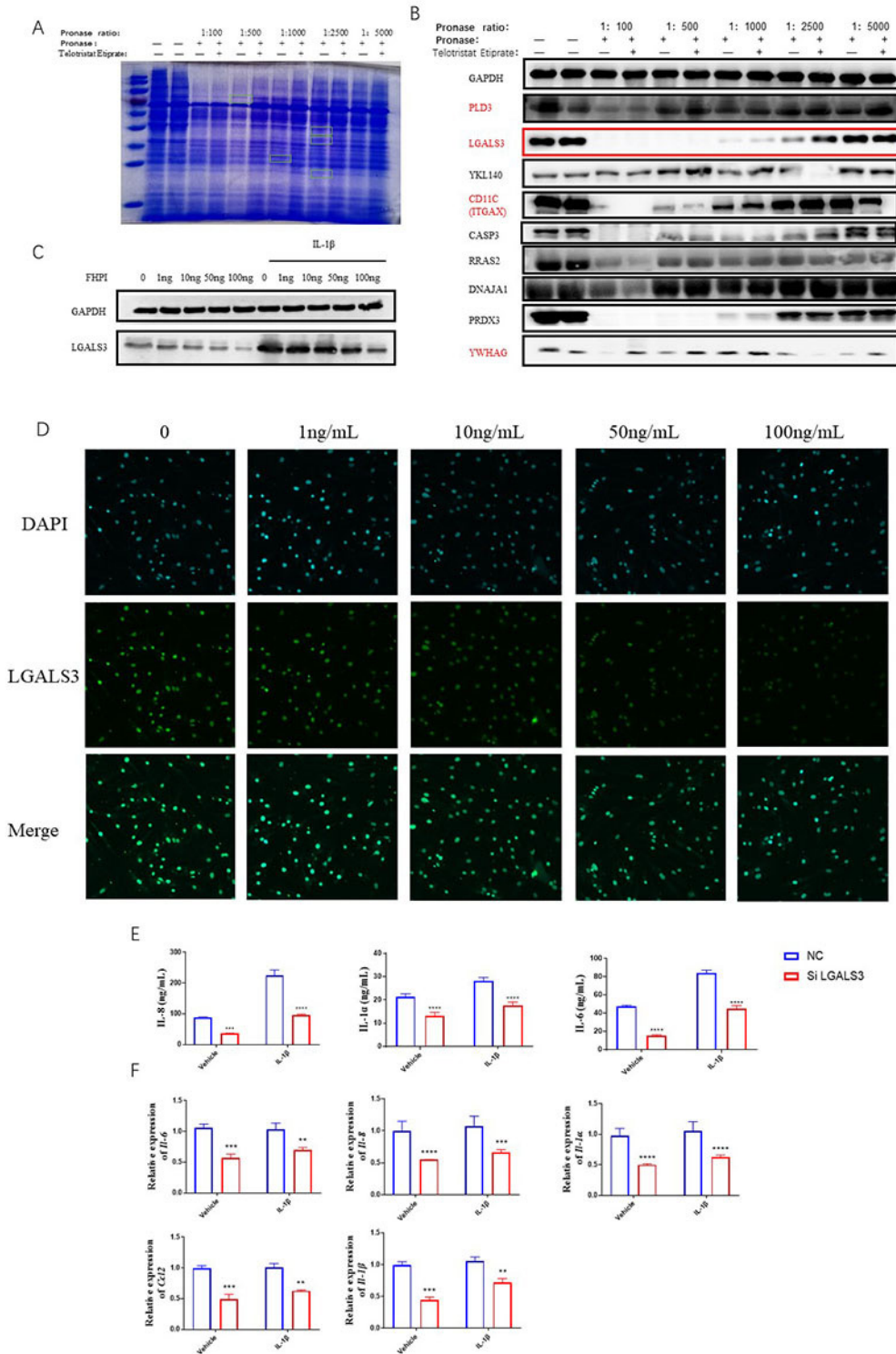


**Figure 4. Telotristat Etiprate affects MAPK signaling by inhibiting UBE2L6.** (A) qRT-PCR was used to verify the significant differentially expressed genes in RNA-SEQ sequencing results. (B) Western blot was used to investigate the effects of Telotristat Etiprate on phosphorylation of MAPK and NF- $\kappa$ B signaling pathways. (C) Silencing genes related to MAPK signaling pathway and detecting its effect on the expression of inflammatory cytokines in cells. (D) and (E) The effects of UBE2L6 silencing and adenovirus overexpression on the expression and secretion of inflammatory cytokines in cells were investigated by ELISA. (F) Western blot analysis of the phosphorylation of MAPK signaling pathway by UBE2L6 silencing and adenovirus overexpression. All results are presented as the mean  $\pm$  SEM of three independent experiments performed in triplicate; \* $p$  < 0.05, \*\* $p$  < 0.01, \*\*\* $p$  < 0.001.



fail to produce the desired therapeutic effect (19-21). In short, we can develop drugs to treat RA using models that predict multiple drug-target interactions.

Telotristat Etiprat is a tryptophan hydroxylase (TPH) inhibitor used in the treatment of carcinoid syndrome. Many neuroendocrine tumors secrete

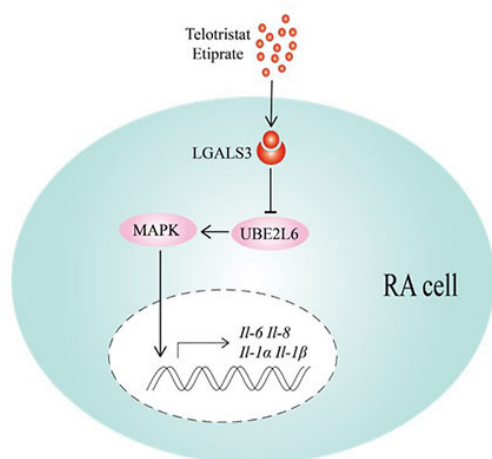


**Figure 6. Telotristat Etiprate can improve RA by inhibiting UBE2L6 expression and affecting the MAPK signaling pathway after targeted binding with LGALS3.**

5-hydroxytryptamine (5-HT) into the bloodstream, causing many symptoms, especially diarrhea. Telotristat Etiprat inhibits TPH, thus reducing the production of 5-HT (22). It has been reported that mice lacking 5-HT transporter (SERT; SERTKO mice) inactivated 5-HT and were oversensitive to both experimentally induced colitis and spontaneous colitis due to interleukin-10 (IL-10) deficiency (23,24). In contrast, mice deficient in tryptophan hydroxylase (TPH1), the rate-limiting enzyme for 5-HT biosynthesis by intestinal chromaffin cells, were resistant to experimentally induced colitis. Thus, when these mechanisms, or the resulting inflammation, become overactive or dysfunctional, it may be advantageous for intestinal chromaffin cells depleted of serotonin to decouple the serotonin drive to inflammation. In addition, serotonin is thought to have a pro-inflammatory effect in animal models. When administered with a reversible inhibitor of tryptophan hydroxylase, a rate-limiting enzyme synthesized by serotonin, inflammation in arthritis-induced mice was significantly reduced by 30-40% (25). In this study, Telotristat Etiprat treatment reduced the invasion and migration ability of RASFs, induced apoptosis of cells, and also inhibited the expression of inflammatory cytokines. Telotristat Etiprat significantly improved joint swelling and erosion in mice in a collagen-induced arthritis (CIA) model. However, through RNA-SEQ and mass spectrometry sequencing results, we found that Telotristat Etiprat could target LGALS3 to inhibit UBE2L6 expression in RA, thereby affecting the MAPK signaling pathway and alleviating RA.

Galectins-3 (LGALS3) is controversial in terms of proinflammatory or anti-inflammatory activity, depending on a variety of factors, including its intracellular or extracellular localization and the target cells involved in these processes (26). Although it may help with inflammation by clearing apoptotic neutrophils, it exhibits pro-inflammatory effects primarily by

enhancing the activation of macrophages, Dendritic cells, mast cells, natural killer cells, and T and B lymphocytes (27). LGALS3 is considered a pro-inflammatory mediator in both RA patients and animal models. LGALS3 mRNA and protein were detected in synovium, while LGALS3 binding protein was mainly expressed at the site of bone destruction (28). RASFs express high levels of CD51 and CD61 integrins, which bind to cartilage oligomeric matrix proteins alone or by forming  $\alpha V\beta 3$  complex (Vitronectin receptor) to induce LGALS3 secretion (29). The externalization of this lectin affects the morphology and persistence of joint inflammation by inducing local fibroblasts to secrete pro-inflammatory cytokines (including IL-6, GM-CSF and MMP-3) and chemokines (such as CCL2, CXCL8, CCL3 and CCL5) (30). LGALS3 stimulates RASF's secretion of IL-6, mediated by Toll-like receptors -2, -3, and -4, amplifying the pro-inflammatory effect (31). In this study, Telotristat Etiprat was found to have a protective effect on LGALS3, and silencing LGALS3 reduced the expression and secretion of inflammatory cytokines in RASFs. These results suggest that LGALS3 can be used as a new target of Telotristat Etiprat to improve RA. In addition, LGALS3 is related to the MAPK signaling pathway (32), which corresponded with our RNA-seq sequencing analysis results, further indicating that Telotristat Etiprat could affect the MAPK signaling pathway by binding to LGALS3.

UBE2L6, an E2 ubiquitin/ISG15 binding enzyme, plays a decisive role in targeting c-MyC proteasome degradation by interacting with E3 ubiquitin ligase, thereby inhibiting cell proliferation and xenograft tumor growth (33). After Telotristat Etiprat treatment, transcriptome sequencing analysis showed that the expression of UBE2L6 was most significantly decreased in RASFs, and the MAPK signaling pathway was phosphorylated, suggesting that Telotristat Etiprat may affect the MAPK signaling pathway by inhibiting UBE2L6 expression. To confirm this idea, we found that the expression and secretion of inflammatory cytokines (IL-6, IL-8, IL-1 $\alpha$ , IL-1 $\beta$ , CCL2) in cells can be inhibited/promoted by silencing and adenovirus overexpression of UBE2L6. In addition, UBE2L6 silencing or adenovirus overexpression can also lead to phosphorylation of the MAPK signaling pathway. Therefore, we believe that Telotristat Etiprat can inhibit the expression of UBE2L6 by combining with LGALS3, thus affecting MAPK signaling pathway and improving RA (Figure 6).

In conclusion, this study found that Telotristat Etiprat may play a certain role in improving RA (by inhibiting the expression and secretion of inflammatory cytokines in cells, inhibiting invasion and migration, inhibiting angiogenesis, and inducing apoptosis). In addition, through RNA-SEQ and mass spectrometry analysis, we found that Telotristat Etiprat could inhibit UBE2L6 expression and affect the MAPK signaling pathway

through targeted binding with LGALS3, thus improving RA.

**Funding:** This work was supported by grants from the National Natural Science Foundation of China (grant no. 81671624), the Key program of Shandong Province (grant no. 2017GSF218082).

**Conflict of Interest:** The authors have no conflicts of interest to disclose.

## References

- Ganesan R, Rasool M. Fibroblast-like synoviocytes-dependent effector molecules as a critical mediator for rheumatoid arthritis: Current status and future directions. *Int Rev Immunol*. 2017; 36:20-30.
- You S, Koh JH, Leng L, Kim WU, Bucala R. The tumor-like phenotype of rheumatoid synovium: Molecular profiling and prospects for precision medicine. *Arthritis Rheumatol*. 2018; 70:637-652.
- Bottini N, Firestein GS. Duality of fibroblast-like synoviocytes in RA: Passive responders and imprinted aggressors. *Nat Rev Rheumatol*. 2013; 9:24-33.
- Lefevre S, Kneda A, Tennie C, *et al*. Synovial fibroblasts spread rheumatoid arthritis to unaffected joints. *Nat Med*. 2009; 15:1414-1420.
- Baier A, Meineckel I, Gay S, Pap T. Apoptosis in rheumatoid arthritis. *Curr Opin Rheumatol*. 2003; 15:274-279.
- Lafyatis R, Remmers EF, Roberts AB, Yocum DE, Sporn MB, Wilder RL. Anchorage-independent growth of synoviocytes from arthritic and normal joints. Stimulation by exogenous platelet-derived growth factor and inhibition by transforming growth factor-beta and retinoids. *J Clin Invest*. 1989; 83:1267-1276.
- Rana AK, Li Y, Dang Q, Yang F. Monocytes in rheumatoid arthritis: Circulating precursors of macrophages and osteoclasts and, their heterogeneity and plasticity role in RA pathogenesis. *Int Immunopharmacol*. 2018; 65:348-359.
- Wang L, Song G, Zheng Y, Wang D, Dong H, Pan J, Chang X. miR-573 is a negative regulator in the pathogenesis of rheumatoid arthritis. *Cell Mol Immunol*. 2016; 13:839-849.
- Smolen JS, Landewe R, Breedveld FC, *et al*. EULAR recommendations for the management of rheumatoid arthritis with synthetic and biological disease-modifying antirheumatic drugs: 2013 update. *Ann Rheum Dis*. 2014; 73:492-509.
- Feely MG. New and emerging therapies for the treatment of rheumatoid arthritis. *Open Access Rheumatol*. 2010; 2:35-43.
- Liu Q, Yang Q, Sun W, *et al*. Discovery and characterization of novel tryptophan hydroxylase inhibitors that selectively inhibit serotonin synthesis in the gastrointestinal tract. *J Pharmacol Exp Ther*. 2008; 325:47-55.
- Kulke MH, Horsch D, Caplin ME, *et al*. Telotristat Ethyl, a Tryptophan Hydroxylase Inhibitor for the Treatment of Carcinoid Syndrome. *J Clin Oncol*. 2017; 35:14-23.
- Pavel M, Gross DJ, Benavent M, *et al*. Telotristat ethyl in carcinoid syndrome: safety and efficacy in the TELECAST phase 3 trial. *Endocr Relat Cancer*. 2018; 25:309-322.
- Aletaha D, Smolen JS. Diagnosis and management of rheumatoid arthritis: A review. *JAMA*. 2018; 320:1360-1372.
- Burmester GR, Pope JE. Novel treatment strategies in rheumatoid arthritis. *Lancet*. 2017; 389:2338-2348.
- Sokka T, Kautiainen H, Mottonen T, Hannonen P. Work disability in rheumatoid arthritis 10 years after the diagnosis. *J Rheumatol*. 1999; 26:1681-1685.
- Boletto G, Kanagaratnam L, Drame M, Salmon JH. Safety of combination therapy with two bDMARDs in patients with rheumatoid arthritis: A systematic review and meta-analysis. *Semin Arthritis Rheum*. 2019; 49:35-42.
- Chen SJ, Lin GJ, Chen JW, Wang KC, Tien CH, Hu CF, Chang CN, Hsu WF, Fan HC, Sytwu HK. Immunopathogenic mechanisms and novel immune-modulated therapies in rheumatoid arthritis. *Int J Mol Sci*. 2019; 20:1332.
- Xiao-Pei H, Ji-Kuai C, Xue W, Dong YF, Yan L, Xiao-Fang Z, Ya-Min P, Wen-Jun C, Jiang-Bo Z. Systematic identification of Celastrol-binding proteins reveals that Shoc2 is inhibited by Celastrol. *Biosci Rep*. 2018; 38:BSR20181233.
- Lin YJ, Liang WM, Chen CJ, Tsang H, Chiou JS, Liu X, Cheng CF, Lin TH, Liao CC, Huang SM, Chen J, Tsai FJ, Li TM. Network analysis and mechanisms of action of Chinese herb-related natural compounds in lung cancer cells. *Phytomedicine*. 2019; 58:152893.
- Boezio B, Audouze K, Ducrot P, Taboureau O. Network-based Approaches in Pharmacology. *Mol Inform*. 2017; 36. doi: 10.1002/minf.201700048.
- Markham A. Telotristat ethyl: First global approval. *Drugs*. 2017; 77:793-798.
- Haub S, Ritze Y, Bergheim I, Pabst O, Gershon MD, Bischoff SC. Enhancement of intestinal inflammation in mice lacking interleukin 10 by deletion of the serotonin reuptake transporter. *Neurogastroenterol Motil*. 2010; 22:826-834, e229.
- Bischoff SC, Mailer R, Pabst O, Weier G, Sedlik W, Li Z, Chen JJ, Murphy DL, Gershon MD. Role of serotonin in intestinal inflammation: knockout of serotonin reuptake transporter exacerbates 2,4,6-trinitrobenzene sulfonic acid colitis in mice. *Am J Physiol Gastrointest Liver Physiol*. 2009; 296:G685-G695.
- Harbuz MS, Perveen-Gill Z, Lalies MD, Jessop DS, Lightman SL, Chowdrey HS. The role of endogenous serotonin in adjuvant-induced arthritis in the rat. *Br J Rheumatol*. 1996; 35:112-116.
- Yang RY, Rabinovich GA, Liu FT. Galectins: structure, function and therapeutic potential. *Expert Rev Mol Med*. 2008; 10:e17.
- Sciacchitano S, Lavra L, Morgante A, Ulivieri A, Magi F, De Francesco GP, Bellotti C, Salehi LB, Ricci A. Galectin-3: One Molecule for an Alphabet of Diseases, from A to Z. *Int J Mol Sci*. 2018; 19:379.
- Ohshima S, Kuchen S, Seemayer CA, Kyburz D, Hirt A, Klinzing S, Michel BA, Gay RE, Liu FT, Gay S, Neidhart M. Galectin 3 and its binding protein in rheumatoid arthritis. *Arthritis Rheum*. 2003; 48:2788-2795.
- Neidhart M, Zaucke F, von Knoch R, Jungel A, Michel BA, Gay RE, Gay S. Galectin-3 is induced in rheumatoid arthritis synovial fibroblasts after adhesion to cartilage oligomeric matrix protein. *Ann Rheum Dis*. 2005; 64:419-424.

30. Filer A, Bik M, Parsonage GN, *et al.* Galectin 3 induces a distinctive pattern of cytokine and chemokine production in rheumatoid synovial fibroblasts *via* selective signaling pathways. *Arthritis Rheum.* 2009; 60:1604-1614.
31. Arad U, Madar-Balakirski N, Angel-Korman A, Amir S, Tzadok S, Segal O, Menachem A, Gold A, Elkayam O, Caspi D. Galectin-3 is a sensor-regulator of toll-like receptor pathways in synovial fibroblasts. *Cytokine.* 2015; 73:30-35.
32. Tian L, Huang CK, Ding F, Zhang R. Galectin-3 mediates thrombin-induced vascular smooth muscle cell migration. *Front Cardiovasc Med.* 2021; 8:686200.
33. Chen Y, Zhou C, Ji W, Mei Z, Hu B, Zhang W, Zhang D, Wang J, Liu X, Ouyang G, Zhou J, Xiao W. ELL targets c-Myc for proteasomal degradation and suppresses tumour

growth. *Nat Commun.* 2016; 7:11057.

Received November 16, 2022; Revised January 31, 2023;  
Accepted February 9, 2023.

§These authors contributed equally to this work.

\*Address correspondence to:

Jihong Pan, Biomedical Sciences College & Shandong Medicinal Biotechnology Centre, Shandong First Medical University & Shandong Academy of Medical Sciences, 6699 Qingdao Road, Ji'nan 250062, China.

E-mail: panjihong@sdfmu.edu.cn

Released online in J-STAGE as advance publication February 11, 2023, 2023.